Proceedings of the
2005 IEEE Conference on Control Applications
Toronto, Canada, August 28-31, 2005

High Precision Feedback Control Design for Dual-Actuator Systems

Tielong Shen and Minyue Fu

Abstract— **Dual-actuator control systems are designed by piggybacking a small secondary actuator onto a primary actuator. Yet the control design for such systems is challenging due to the limited dynamic range of the secondary actuator and its coupling with the primary actuator. In this paper, we propose a new control design approach for dual-actuator systems. We first show that, through a simple coordinate transformation, a dual-actuator system can be separated into two subsystems, one of them controlled only by the primary actuator, which can be designed using conventional methods, and the other one involving tracking control using the secondary actuator. We then devise a switching control strategy for the secondary actuator to achieve high precision control. Two dual-actuator systems are used to demonstrate the use of dual actuators and effectiveness of the new design approach.**

I. INTRODUCTION

The structural characteristic of a dual-actuator system is that there are two cascaded actuators operating along a common axis. The primary actuator, called *primary actuator*, is of long range but with poor accuracy and slow response time. The minor actuator, called *secondary actuator*, is typically piggybacked onto the primary actuator and delivers much higher precision and faster response but has a limited dynamic range. A good example of dual-actuator systems is the so-called dual-stage hard disk drive servo system which consists of a voice coil motor as the primary actuator and a piezo-electric transducer as the secondary actuator [1]-[2]. Other examples include VLSI chip manufacturing machines [3], [4] and high precision machining tools [5], [6].

Although the mechanical design of dual-actuator systems appears to be simple and the functionalities of each actuator appear to be qualitatively clear, it is a challenging task to coordinate the two actuators to yield an optimal performance. The main obstacle is that secondary actuator typically has a very limited motion range. A naive design approach is to tune the primary actuator to achieve a rough positioning or tracking and then to activate the secondary actuator when the primary actuator reaches its steady state. This approach appears to make sense because the secondary actuator does not have much influence when the tracking error is large; and conversely, the secondary actuator should take over when the primary actuator has exhausted its ability to reduce the tracking error. However, such an approach is inadequate for at least two reasons: 1) The overall response time is typically excessively long; 2) In many applications the system is subject to disturbances or the tracking reference signal is time-varying, which implies that the primary actuator can never be in a steady state. Many other design approaches also exist. For example, a common design approach for dual-stage hard disk drive systems is to design two separate control loops, one for each actuators by assuming that the interaction between the two control loops is negligible. The two loops can operate in either series [7] or parallel [8]. In such a design, the primary and secondary actuators are assigned to control low and frequency responses, respectively. However, it is well known that this control approach typically results in poor stability performance due to the coupling between the two actuators. Indeed, the most difficult aspect of the dual-actuator control design is to figure out how to coordinate the two actuators in a region where both actuators have some but limited control authorities.

In this paper, we propose a new control design approach for dual-actuator systems. Our research starts with an interesting observation that many dual-actuator systems can be effectively decoupled through a simple coordinate transformation. The result of it is that we have two subsystems, a *primary system* and a *secondary system* behaving as follows. The primary system is approximately independent of the secondary system and is purely driven by the primary actuator. The controller of the primary system can be designed using standard means, and thus is not of primary interest. On the other hand, the secondary system is controlled by the secondary actuator and the coupling from the primary system is only through the reference signal for positioning or tracking. Motivated by the observation above, we then focus on the control design for the secondary actuator. Modeling the secondary actuator as a saturated controller, this problem can be casted as a tracking control problem with an input saturation. Existing design approaches range from anti-windup compensators [9]-[10] to Riccati equation or linear matrix inequality based approaches [11]-[13]. In our design approach, we choose to optimize a quadratic performance function. To get around the difficulty with the input saturation, we exploit a switching control strategy which applies different control gains when the state of the system lie in different regions. These regions are characterized by nested ellipsoids with outer ellipsoids corresponding to looser performance bounds and the inner ones to tighter bounds. As the tracking error converges, the controller gradually switches from low performance gains to high performance ones. Two design examples are used to demonstrate our design approach. The first one is a simple two-mass system exemplifying a single-axis linear-motion dual-actuator system. The second one is a dual-stage synchronization system commonly used in the micro-manufacturing industry.

Tielong Shen is with the Department of Mechanical Engineering, Sophia University, Kioicho 7-1, Chiyoda-ku, Tokyo 102-8554, Japan.
Minyue Fu is with the School of Electrical Engineering and Computer Science, The University of Newcastle, Callaghan, NSW 2308, Australia.

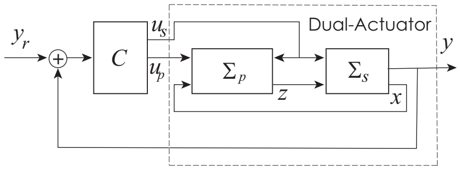

Fig. 1. Typical Dual-Actuator Control System

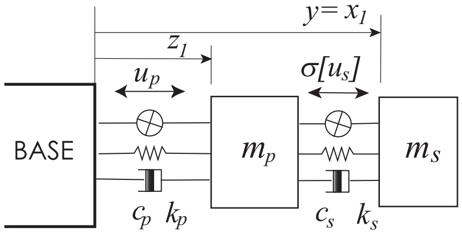

Fig. 2. A two-mass model for Dual-Actuator Systems (Linear Motion)

II. Modeling of dual-actuator systems

A dual-actuator system can be depicted in Fig. 1, where Σ_p and Σ_s denote the primary and secondary systems (or subsystems), respectively. The primary actuator u_p drives the primary system directly and the secondary actuator u_s controls the secondary system but it also injects a counter-action directly onto the primary system. The state vectors of the two subsystems are denoted by x and z, respectively. The control objective is to design a suitable controller $\mathcal{C}$ such that the output y of the secondary system tracks a given reference signal y_r with some prescribed performance specifications.

A dual-actuator system with single-axis linear motion can be represented by a two-mass model as shown in Fig. 2. The mass, damping coefficient, spring constant, position and velocity of the primary system are denoted by m_p, c_p, k_p, z_1 and z_2 respectively. Their counterparts for the secondary system are denoted by m_s, c_s, k_s, x_1 and x_2, respectively. The output y equals x_1. In this model, the primary system is attached to a fixed base. However, additional dynamics to the base and the interactions with them can be modeled into the actuating function u_p. The dynamic equations of the system are given as follows:

$$\begin{cases} \dot{x}_1 = x_2 \\ \dot{z}_1 = z_2 \\ m_p\dot{z}_2 = u_p - \sigma[u_s] - c_p z_2 - k_p z_1 + f(x_1, x_2, z_1, z_2) \\ m_s\dot{x}_2 = \sigma[u_s] - f(x_1, x_2, z_1, z_2) \end{cases} \tag{1}$$

where $f(x_1, x_2, z_1, z_2) = c_s(x_2 - z_2) + k_s(x_1 - z_1 - l_0)$ represents the interaction force between two actuators, $l_0 > 0$ denotes the offset distance between two masses, and $\sigma[\cdot]$ is a saturation function defined by

$$\sigma[u] = \begin{cases} a & (u > a) \\ u & (|u| \le a) \qquad a > 0 \\ -a & (u < -a) \end{cases} \tag{2}$$

Next, we show that the model (1) can be decoupled into two subsystems via a simple coordinate transformation. This is motivated by the fact that the primary system typically has a much larger mass than the secondary system. Let

$$z_1 \to \xi_1 = \frac{m_s x_1 + m_p z_1}{m_s + m_p}, \quad z_2 \to \xi_2 = \dot{\xi}_1 \tag{3}$$

That is, we choose the mass center ξ_1 and its derivative as a new coordinate for the primary system. It follows that

$$\dot{\xi}_2 = bu_p(t) - a_2\xi_2(t) - a_1\xi_1(t) + \epsilon(t) \tag{4}$$

where $b = (m_s + m_p)^{-1}, a_1 = k_p m_s m_p^{-1}, a_2 = c_p m_s m_p^{-1}$ and $\epsilon(t) = m_s(k_s x_1 + c_s x_2)/(m_p^2 + m_s m_p)$ describes the coupling force from the motion of the secondary system. Due to the fact that $m_p \gg m_s$, we can simply ignore the $\epsilon(t)$ term. It follows that the dynamics of the primary system is approximately decoupled from that of the secondary system and the design of $u_p(t)$ can be done using any conventional method.

On the other hand, if we define $e_1 = x_1 - y_r$ and $e_2 = \dot{e}_1 = x_2 - \dot{y}_r$, then

$$\dot{e}_2 = g\{\sigma[u_s(t)] - d(t)\} - h_2 e_2(t) - h_1 e_1(t) \tag{5}$$

where $g = m_s^{-1}, h_1 = k_s m_s^{-1}, h_2 = c_s m_s^{-1}$ and

$$d(t) = c_s(\dot{y}_r - z_2) + k_s[r - (z_1 + l_0)] + m_s\ddot{y}_r. \tag{6}$$

The model (5) now becomes the model for the secondary system. We observe that the coupling signal $d(t)$ is dominated by the error between the state of the primary actuator (z_1, z_2) and the desired state $(y_r - l_0, \dot{y}_r)$ and the acceleration command $m_s\ddot{y}_r$. If the error or the acceleration command is large, it is not possible to completely compensate $d(t)$ by using $u_s(t)$. It is only when $d(t)$ is within a small region (in comparison with a) that the secondary actuator has some meaningful control effect.

The observation above means the following. We can use the input of the primary actuator to drive the mass center such that the new reference signal $d(t)$ converges to a small region as quickly as possible. Prior to such convergence of $d(t)$, the secondary actuator should be turned off because it does not have much effect. The control gain of $u_s(t)$ should be gradually increased when $d(t)$ becomes small. This motivates the idea of a switching control strategy for the secondary actuator, which we discuss in the next two sections.

III. Control design for secondary actuator

In this section, we focus on the design problem for the secondary system in a dual-actuator system. In view of the discussions in Section II, we consider the following model:

$$\dot{x} = Ax + b(\sigma[u] - d(t)), \quad x(0) = x_0 \tag{7}$$

where $x \in I\!R^n$ is the state with initial condition x_0, $u \in I\!R$ is the control input, $d(t) \in I\!R$ is a given reference signal, and $A \in I\!R^{n\times n}$ and $b \in I\!R^{n\times 1}$ are given. Without loss of generality, we assume that the saturation level is $a = 1$.

Roughly speaking, the design goal is to find a state feedback control law such that the state x is driven from its initial state $x(0)$ to the origin with a pre-specified performance cost or less and that the region of such initial state is maximal.

It is obvious that if $|d(t)| > 1$ holds persistently, it is not possible to achieve the design goal. Therefore, it is necessary for the primary actuator the bring the steady state value of $d(t)$ to be within $[-1,\ 1]$. In view of this, we assume that the control action of the primary actuator has been applied prior to $t = 0$ such that $|d(t)| \le d_0,\ \forall t \ge 0$ for some $d_0 \in (0,\ 1)$.

Under the assumption, we can compensate the disturbance by introducing a feed-forward term in $u(t)$ as follows:

$$u(t) = v(t) + d(t) \tag{8}$$

Then we can rewrite (7) as

$$\dot{x} = Ax + b\sigma_d[v], \quad x(0) = x_0 \tag{9}$$

where $\sigma_d[\cdot]$ is defined as in (2) with $a = 1 - d(t) > 0$.

We now consider the following quadratic cost function

$$J(x_0, v) = \int_0^\infty \{x^T Q x + r\sigma_d^2[v]\} dt \tag{10}$$

for some $Q = Q^T \ge 0$ and $r > 0$ with $(A, Q^{\frac{1}{2}})$ being detectable, where $\sigma_d[v] = \sigma[u] - d(t)$. We seek to minimize $J(x_0, v)$ by using a linear state feedback $v = Kx$. If there is no saturation, it is well-known that the optimal solution for v is given by

$$v^* = -r^{-1} b^T P_0 x \tag{11}$$

and the minimum quadratic cost is $x_0^T P_0 x_0$, where $P_0 = P_0^T > 0$ is the solution to the following Riccati equation:

$$A^T P_0 + P_0 A + Q - r^{-1} P_0 b b^T P_0 = 0 \tag{12}$$

In the presence of saturation, the optimal v is difficult to compute. To get around this difficulty, we follow the approach in [12] by parameterizing the controller by using a bound on v. More precisely, given $\rho \ge 0$, we restrict the v to be such that

$$|v| \le \rho + (1 - d_0) \tag{13}$$

That is, ρ acts as an *over-saturation bound*. It is easy to verify that for any v constrained by (13), $\sigma_d[v]$ lies in the following sector bound as shown in Fig. 3

$$\delta(v) = \sigma_d[v] - \rho_1 v; \quad |\delta(v)| \le \rho_2 |v| \tag{14}$$

where

$$\rho_1 = \frac{2(1 - d_0) + \rho}{2(1 - d_0 + \rho)}, \quad \rho_2 = \frac{\rho}{2(1 - d_0 + \rho)} \tag{15}$$

Now, for a given $\rho > 0$, consider a Lyapunov function candidate of the form $V(x) = x^T P_\rho x$ for some $P_\rho = P_\rho^T$ to be determined and define

$$\Omega_\rho = A^T P_\rho + P_\rho A + Q - r^{-1} P_\rho b b^T P_\rho \tag{16}$$

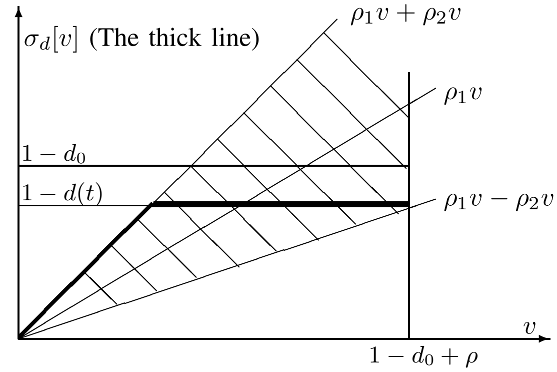

Fig. 3. Sector Bound for $\sigma_d[v]$

It is straightforward to verify that

$$\begin{aligned} J(x_0, v) &= \lim_{T\to\infty} V(x_0) - V(x(T)) \\ &\quad + \int_0^\infty (\dot{V} + x^T Q x + r\sigma_d^2[v]) dt \\ &\le V(x_0) + \int_0^\infty \varphi(x, v, \delta(v)) dt \end{aligned}$$

where

$$\begin{aligned} \varphi(x, v, \delta(v)) &= x^T (A^T P_\rho + P_\rho A + Q) x \\ &\quad + r\sigma_d^2[v] + 2x^T P_\rho b \sigma_d[v] \\ &= x^T \Omega_\rho x + r(\rho_1 v + \delta(v) - v^*)^2 \end{aligned} \tag{17}$$

This implies that if $\varphi(x, v, \delta(v)) \le 0$ along the trajectory of the system (9) with the feedback control, we have

$$J(x_0, v) \le V(x_0) \tag{18}$$

Using the analysis above, we formulate the following (relaxed) *auxiliary optimal control problem*: For a given $\rho \ge 0$, design P_ρ and v to minimize $V(x_0)$ subject to $\varphi(x, v, \delta(v)) \le 0$ for all $x \in \mathbf{R}^n$ and all $\delta(\cdot)$ satisfying the following sector bound:

$$|\delta(v)| \le \rho_2 |v| \tag{19}$$

In addition, determine the largest invariant set of the form

$$X_\rho = \{x : x^T P_\rho x \le \mu_\rho^2\} \tag{20}$$

such that for any $x_0 \in X_\rho$, $x(t) \in X_\rho$ and $|v(t)| \le 1 - d_0 + \rho$ for all $t \ge 0$ and $J(x_0, v) \le V(x_0)$.

Theorem 1: Consider the system in (9), the quadratic cost function in (10) and a given bound $\rho \ge 0$ on the level of over-saturation. Define $\rho_0 = \rho_2/\rho_1$. Suppose the equation

$$A^T P_\rho + P_\rho A - r^{-1}(1 - \rho_0^2) P_\rho b b^T P_\rho + Q = 0 \tag{21}$$

has a solution $P_\rho > 0$. Then the optimal K_ρ and the associated X_ρ for the auxiliary optimal control problem are given by

$$K_\rho = -\rho_1^{-1} r^{-1} b^T P_\rho \tag{22}$$

$$\mu_\rho = \frac{2(1 - d_0) + \rho}{2\sqrt{b^T P_\rho b}} r \tag{23}$$

Proof: We first solve

$$\min_{v} \max_{|\delta(v)|\leq\rho_2|v|} \varphi(x,v,\delta(v))$$

for a given $x \in I\!R^n$. It is straightforward to compute

$$\begin{aligned}&\max_{|\delta(v)|\leq\rho_2|v|} \varphi(x,v,\delta(v))\\ = \quad & x^T\Omega_\rho x + r\{(\rho_1 v - v^*)^2 + 2\rho_2|(\rho_1 v - v^*)v| + \rho_2^2 v^2\}\end{aligned}$$

where $v^* = -r^{-1}b^T P_\rho x$. We consider two cases: 1) $\rho_1 v^2 \geq v^* v$ and 2) $\rho_1 v^2 \leq v^* v$. For the first case, we have

$$\begin{aligned}&\max_{|\delta(v)|\leq\rho_2|v|} \varphi(x,v,\delta(v))\\ = \quad & x^T\Omega_\rho x + r\{(\rho_1 v - v^*)^2 + 2\rho_2(\rho_1 v - v^*)v + \rho_2^2 v^2\}\\ = \quad & x^T\Omega_\rho x + r(v-v^*)^2\end{aligned}$$

The last step is obtained by using $\rho_1 + \rho_2 = 1$. The minimizing v subject to $\rho_1 v^2 \geq v^* v$ is given by $v = \rho_1^{-1}v^*$, then

$$\begin{aligned}&\min_{v:\rho_1 v^2\geq v^* v} \max_{|\delta(v)|\leq\rho_2|v|} \varphi(x,v,\delta(v))\\ = \quad & x^T\Omega_\rho x + r(\rho_1^{-1}v^* - v^*)^2\\ = \quad & x^T\Omega_\rho x + r\rho_2^2\rho_1^{-2}(v^*)^2 = x^T\tilde{\Omega}_\rho x\end{aligned}$$

where $\tilde{\Omega}_\rho = A^T P_\rho + P_\rho A + Q - (1-\rho_0^2)P_\rho b b^T P_\rho$. For the second case, we have

$$\begin{aligned}&\max_{|\delta(v)|\leq\rho_2|v|} \varphi(x,v,\delta(v))\\ = \quad & x^T\Omega_\rho x + r\{(\rho_1 v - v^*)^2 - 2\rho_2(\rho_1 v - v^*)v + \rho_2^2 v^2\}\\ = \quad & x^T\Omega_\rho x + r((\rho_1-\rho_2)v - v^*)^2\end{aligned}$$

It follows that

$$\begin{aligned}&\min_{v:\rho_1 v^2\leq v^* v} \max_{|\delta(v)|\leq\rho_2|v|} \varphi(x,v,\delta(v))\\ = \quad & x^T\Omega_\rho x + r((\rho_1-\rho_2)\rho_1^{-1}v^* - v^*)^2\\ = \quad & x^T\Omega_\rho x + r\rho_2^2\rho_1^{-2}(v^*)^2 = x^T\tilde{\Omega}_\rho x\end{aligned}$$

with the same optimal v. Hence, we conclude that the optimal v is $\rho_1^{-1}v^*$ which is the same as (22). From the above discussion, we know that given x and v,

$$\max_{|\delta(v)|\leq\rho_2|v|} \varphi(x,v,\delta(v)) \leq x^T\tilde{\Omega}_\rho x + \Delta(x,v)$$

where $\Delta(x,v) \geq 0$ with $\Delta(x,\rho_1^{-1}v^*) = 0$.

Next, we need to minimize $x_0^T P_\rho x_0$ subject to

$$x^T\tilde{\Omega}_\rho x + \Delta(x,v) \leq 0$$

or equivalently,

$$x^T\tilde{\Omega}_\rho x \leq -\Delta(x,v)$$

We note that the upper bound of $\tilde{\Omega}_\rho$ increases as $\Delta(x,v)$ decreases. Also, P_ρ has a well-known monotonicity, i.e., it decreases when $\tilde{\Omega}_\rho$ increases. Hence, the optimal P_ρ is obtained by minimizing $\Delta(x,v)$ and maximizing $\tilde{\Omega}_\rho$, i.e., by setting v as in (22) and $\tilde{\Omega}_\rho = 0$ which leads to (21).

In order to characterize the invariant set X_ρ, all we need to do is to determine the largest μ_ρ such that

$$\max_{x^T P_\rho x\leq\mu_\rho^2} |Kx| = \left|\rho_1^{-1}r^{-1}B^T P_\rho x\right| = 1 - d_0 + \rho \qquad (24)$$

Let $\eta = P_\rho^{1/2}x$. Then,

$$\max_{x^T P_\rho x\leq\mu_\rho^2} |Kx| = \max_{\|\eta\|\leq\mu_\rho} |r^{-1}\rho_1^{-1}B^T P_\rho^{-1/2}\eta| \qquad (25)$$

The optimizing η is given by

$$\eta_0 = \frac{\mu_\rho}{\|P^{1/2}B\|}P_\rho^{1/2}b \qquad (26)$$

Substituting $x = P_\rho^{-1/2}\eta_0$ into (24), we obtain (23). ∎

Remark 1: If $\rho = 0$, the Riccati equation (21) and the control gain (22) recover the results in (12) and (11) for no saturation. The associated invariant set is given by

$$X_0 := \{x : x^T P_0 x \leq \mu_0\}, \quad \mu_0 = \frac{2(1-d_0)r}{2\sqrt{b^T P_0 b}} \qquad (27)$$

IV. Nested switching control

Roughly speaking, a practical way to avoid or reduce input saturation is to make the controller gain small when the state is large and to increase the gain when the state is small. Switching control with a sequence of nested control laws is motivated by this basic idea. To do this, a sequence of control laws need to be designed in such a way that the invariant sets are nested. More precisely, we need to find the controllers $K_i, i = 0,1,\cdots,N$ such that the corresponding invariant sets $X_i = \{x : x^T P_i x \leq \mu_i^2\}, i = 0,1,\cdots,N$, satisfy $X_0 \subset X_1 \subset \cdots \subset X_N$. Furthermore, we also demand $P_0 < P_1 < \cdots < P_N$ so that the quadratic performance gets improved gradually when the control gain switches from K_N to K_0.

The desired nesting properties above can indeed be achieved by using the design method in the previous section with different values of ρ. This is due to the monotonicity of the Riccati equation (21). Indeed, we can rewrite (21) as

$$A^T S_\rho + S_\rho A - r^{-1}(1+\rho_0)S_\rho B B^T S_\rho + Q_\rho = 0 \qquad (28)$$

where $S_\rho = (1-\rho_0)P_\rho$ and $Q_\rho = (1-\rho_0)Q$. Using S_ρ and Q_ρ, the invariant set (20) can be expressed as

$$\begin{aligned}X_\rho \quad &= \quad \left\{x:\ x^T P_\rho x \leq \frac{(1-d_0)^2 r^2}{(1-\rho_0)b^T S_\rho B}\right\}\\ &= \quad \left\{x:\ x^T S_\rho x \leq \frac{(1-d_0)^2 r^2}{b^T S_\rho B}\right\}\end{aligned} \qquad (29)$$

Theorem 2: The solution S_ρ to equation (28) is monotonically decreasing in $\rho > 0$, i.e., $S_{\rho+\varepsilon} < S_\varepsilon$, if $0 \leq \rho < \rho+\varepsilon$. Consequently, X_ρ has the following nesting property:

$$X_\rho \subset X_{\rho+\varepsilon}, \quad 0 \leq \rho < \rho+\varepsilon \qquad (30)$$

Similarly, we have

$$P_\rho < P_{\rho+\varepsilon}, \quad 0 \leq \rho < \rho+\varepsilon \qquad (31)$$

Proof: It suffices to establish the result above for sufficiently small $\varepsilon > 0$. It is easy to verify that $\rho_0 = \rho/[2(1-$

$d_0)+\rho]$ is monotonically increasing in ρ. Thus, for any $\varepsilon > 0$, we can write

$$\frac{\rho+\varepsilon}{2(1-d_0)+\rho+\varepsilon} = \rho_0 + \varepsilon_1$$

with some $\varepsilon_1 > 0$. It follows that the Riccati equation (28) for $\rho+\varepsilon$ can be represented as

$$\begin{aligned} &A^T S_{\rho+\varepsilon} + S_{\rho+\varepsilon} A - r^{-1}(1+\rho_0+\varepsilon_1) S_{\rho+\varepsilon} BB^T S_{\rho+\varepsilon} \\ &+(1-\rho_0-\varepsilon_1)Q = 0 \end{aligned} \tag{32}$$

Let $E = S_\rho - S_{\rho+\varepsilon}$. From (28) and (32), we have

$$\begin{aligned} &\tilde{A}^T E + E\tilde{A} + +r^{-1}(1+\rho_0+\varepsilon_1) EBB^T E \\ &+\varepsilon_1 Q + \varepsilon_1 S_\rho BB^T S_\rho = 0 \end{aligned} \tag{33}$$

where $\tilde{A} = A - r^{-1}(1+\rho_0+\varepsilon_1)BB^T S_\rho$. From (28), we know that $A - r^{-1}(1+\rho_0)BB^T S_\rho$ is Hurwitz. Therefore, $A - r^{-1}(1+\rho_0+\varepsilon_1)BB^T S_\rho$ is also Hurwitz when ε_1 (or equivalently, ε) is sufficiently small. It follows from (33) and the detectability of $(A, Q^{1/2})$ that $E > 0$, i.e. $S_\rho > S_{\rho+\varepsilon}$. The nesting property of X_ρ then follows from (29).

The monotonicity of P_i is proved similarly. ∎

Based-on the nesting property of the invariant set X_ρ, we can apply Theorem 1 to design a sequence of control gains $K_i (= K_{\rho_i}), i = 0, 1, \cdots, N$, for a sequence of over-saturation bounds $0 = \rho_0 < \rho_1 < \rho_2 < \cdots < \rho_N$, and switch the gain to K_i whenever $x \in X_i (= X_{\rho_i})$ but is outside of $X_{i-1} (= X_{\rho_{i-1}})$. The next result shows the performance improvement by using this switching control.

Theorem 3: Suppose the switching controller above is applied to the system in (9) with $x_0 \in X_N$. Let τ_i be the time instance K_i is switched on, $i = 0, 1, \cdots, N$. In particular, $\tau_N = 0$. Then,

$$J(x_0, v) = x_0^T P_N x_0 - \sum_{i=0}^{N-1} x^T(\tau_i)\Delta P_i x(\tau_i) \tag{34}$$

where $\Delta P_k = P_{i+1} - P_i > 0,\ i = 0, 1, \cdots, N-1$.

Proof: Following the proof of Theorem 1, we have

$$x^T Q x + r\sigma_d^2[K_i x] \le -\frac{d}{dt}\left\{x^T P_i x\right\} \tag{35}$$

along the trajectory of $x(t), t \in [\tau_{i+1}, \tau_i)$. Integrating the inequality above yields (34). ∎

V. DESIGN EXAMPLES

A. Single-axis Dual-Stage Positioning control

Recall the dual-stage positioning system in Fig. 2. The control problem is to drive the output y to a given command y_r. The physical parameters of the system are shown in Table I. The saturation level for the secondary stage is $a = 0.02$ and the offset between the two stages is $l_0 = 0.05$. Rescaling the control input and the input matrix as $0.02u \to u$ and $0.02B \to B$, the system can be rewritten as model (1) with the saturation level $a = 1$. Choose Q and r as

$$Q = \begin{bmatrix} 50 & 0 \\ 0 & 10 \end{bmatrix}, \quad r = 0.1 \tag{36}$$

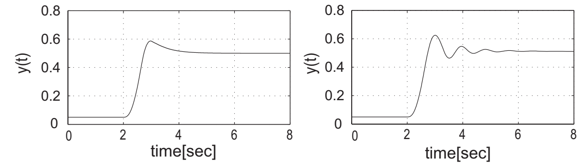

Fig. 4. Time response ($y(t)[m]$)

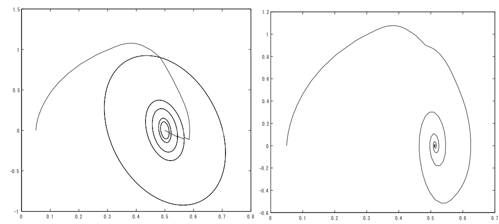

Fig. 5. State trajectories

In order to show the effectiveness of the nested switching control strategy, we are mainly interested in the control design for the secondary stage. The primary actuator is simply controlled by a PID controller with the gains $k_p = 50.0, \quad k_I = 5, \quad k_d = 0$.

To design the secondary stage, we take $d_0 = 0.01$ and choose the over-saturation levels to be $\rho_4 = 50, \rho_3 = 10, \rho_2 = 5, \rho_1 = 1$ and $\rho_0 = 0$. This leads to the switching feedback control gains

$$\begin{aligned} K_4 &= [-76.0594 \quad -57.8713] \\ K_3 &= [-50.1572 \quad -30.7876] \\ K_2 &= [-40.1313 \quad -23.2691] \\ K_1 &= [-25.0582 \quad -13.6835] \\ K_0 &= [-17.9129 \quad -9.6805] \end{aligned} \tag{37}$$

The corresponding domains of attraction have $\mu_4 = 1.1450, \mu_3 = 0.1069, \mu_2 = 0.0449, \mu_1 = 0.0108$ and $\mu_0 = 0.0051$. The corresponding Lyapunov matrices for μ_4 and μ_0, for example, are given by, respectively,

$$P_4 = \begin{bmatrix} 28.1408 & 1.9384 \\ 1.9384 & 1.4749 \end{bmatrix}, P_0 = \begin{bmatrix} 24.4199 & 0.8956 \\ 0.8956 & 0.4840 \end{bmatrix}$$

Simulation results are shown in Figs. 4-5 (the left plots) which demonstrate the step response to the set-point command $y_r = 0.5$. The domains of attraction are also shown in Fig. 5. To compare the performance of the proposed switching controller, we also show the response (the right plots in Figs. 4-5) when the secondary stage is controlled by a P controller with "optimized" gains $k_p = 0.45,\ k_i = 0,\ k_d = 0$. It is clear from the simulations that the proposed switching controller can drive the output y to y_r much faster than a PID controller.

B. Synchronizing control of multi-stages

Synchronization of two or more mechanical machines is very important when the machines must cooperate. Stepping-and-laser scanning systems are typical machines of this kind widely used in the semiconductor manufacturing industry.

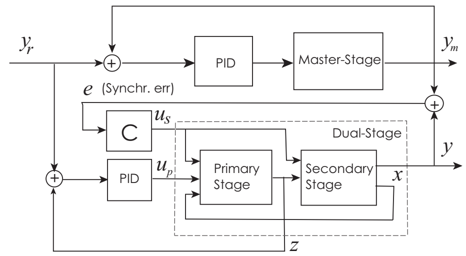

Fig. 6. Synchronizing control system with dual-actuator

Fig. 6 shows a typical setup of such a system. In this setup, a wafer is placed on the master stage (called wafer stage) and a reticle are placed on a slave stage (called reticle stage). The two stages are required to move in synchrony with high precision along the same axis so that the content in the reticle can be exposed to the wafer. In order to achieve the high precision in synchronization, a dual-stage is usually used for the reticle stage. The control of the secondary stage is targeted at tracking the motion of the wafer-stage.

The parameters of the system used in the simulation are shown in Table II. For simplicity, the parameters of the dual-stage system is chosen to be the same as in Example 1. Consequently, the same switching controller for Example 1 is used here. However, the PID controller for the primary stage is adjusted to have $k_p = 100, k_i = 15, k_d = 0$ to improve the synchronizing performance. Two different command signals of y_r, ramp and sine wave, are used in the simulation. The responses of the master stage are shown in Fig. 7 (the plots in the top), and the corresponding synchronization errors are shown in Fig. 7 (the plots in the middle).

To compare the effectiveness of the proposed synchronization approach where the reticle stage is actuated by the dual-stage with the switching controller, we also show in Fig. 7 (the last two plots) the synchronization error when the reticle stage is driven by a single actuator, i.e. the secondary stage is fixed on the primary stage. It is clear from Fig. 7 that the proposed switching controller performs much better.

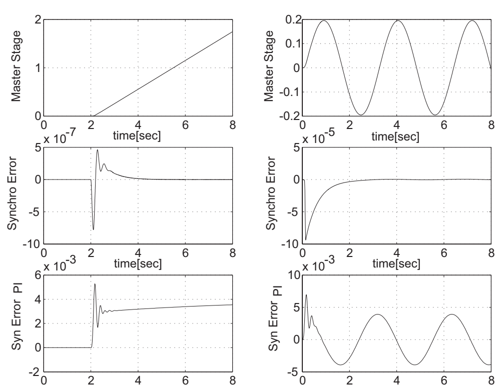

Fig. 7. Synchronization with the proposed control and PID control (the master stage position $y_m(t)[m]$ and the synchronization error $e(t)[m]$)

TABLE I

PHYSICAL PARAMETERS OF THE DUAL-STAGE

	Mass[kg]	Spring[N/m]	Damper[Ns/m]
Primary-Stage	0.1	0.2	0.1
Secondary-Stage	0.01	0.1	0.025

TABLE II

PHYSICAL PARAMETERS OF THE STAGES

	Mass[kg]	Spring[N/m]	Damper[Ns/m]
Master-Stage	0.1	0.7	0.6
Primary-Stage	0.1	0.2	0.1
Secondary-Stage	0.01	0.1	0.025

VI. CONCLUSIONS

For dual-actuator systems, an effective way to achieve fine control quality is to design the control strategy with delicate sensitivity, due to the primary and the secondary actuator have different range and different response properties. Particulary, the secondary actuator is usually saturated and of small range. In this paper, we have shown that a feasible method to this end is to focus the design arm on the secondary actuator, since the control can be decoupled by a simple coordinate change. We proposed a nested switching control approach for the secondary actuator which takes the saturation and the interaction from the primary actuator into account.

REFERENCES

[1] R. B. Evans *et. al.*, "Piezoelectric micro-actuator for dual stage control," *IEEE Trans. Magnetics*, vol. 35, pp. 977-982, 1999.

[2] S. H. Lee, S. E. Baek and Y. H. Kim, "Design of a dual stage actuator control system with discrite-time sliding mode for hard disk drives," *IEEE Conf. Decision and Control*, Sydney, pp. 3120-3125, 2000.

[3] S. Makinouchi, Y. Hayashi and S. Kamiya, New stage system for step-and-repeat scaning stepper, *Transaction of The Japan Society for Precision Engineering*, Vol.61, No.12, pp.1676-1680, 1995.

[4] M. Tomizuka, J.-S. Hu, T.-C. Chin and T. Kamano, Synchronization of Two Motion Control Axes Under Adaptive Feedforward Control, *Journal of Dynamic Systems, Measurement and Control*, Vol.114, No.2, pp.196-203, 1992.

[5] T. Kamano, T. Suzuki, N. Iuchi and M. Tomizuka, Adaptive Feedforward Controller for Synchronization of Two Axes Positioning System, *Transactions of the Society of Instrument and Control Engineers*, Vol.29, No.7, pp.785-791, 1993.

[6] L.-F. Yang and W.-H. Chang, Synchronization of Twin-Gyro Precession Under Cross-Coupled Adaptive Feedforward Control, *Journal of Guidance, Control, and Dynamics*, Vol.19, No.3, pp.534-539, 1996.

[7] S. J. Schhroeck and W. C. Messner, "On control design for time invariant dual-input single-ouput systems," *Proc. American Control Conf.*, pp. 4122-4126, 1999.

[8] S. J. Schhroeck, W. C. Messner and R. J. McNab, "On compasator design for linear time invariant dual-input single-ouput systems," *IEEE Trans. Mechatoronics*, vol. 50-57, Mar. 2001.

[9] W. Niu and M. Tomizuka, "An anti-windup design for the asymptotic tracking of linear system subject to actuator saturation," *Proc. American Control Conf.*, Philadephia, pp. 1458-1462, 1998.

[10] N. Kapoor, A. Teel and P. Daoutidis, "An anti-windup design for linear systems with input saturation," *Automatica*, vol.34,pp.559-574, 1998.

[11] A. Saberi, Z. Lin and A. R. Teel, "Control of linear systems with saturation actuators," *IEEE Trans. Auto. Contr.,*, vol.41, pp.368-378, 1996.

[12] M. Fu, "Linear Quadratic Control with Input Saturation," in *Perspectives in Robust Control*, ed.S.O.R.Moheimani, Springer, 2001.

[13] T. Iwasaki and M. Fu, "Regional H_2 performance synthesis," in *Actuator Saturation Control*, Eds. V. Kapila and K. M. Grigoriadis, Marcel Dekker, Inc., New York, 2001.